

Orbital Switching and the First-Order Insulator-Metal Transition in Paramagnetic V_2O_3

M. S. Laad, L. Craco and E. Müller-Hartmann

Institut für Theoretische Physik, Universität zu Köln, 77 Zùlpicher Strasse, D-50937 Köln, Germany
(February 1, 2008)

The first-order metal-insulator transition (MIT) in paramagnetic V_2O_3 is studied within the ab-initio scheme LDA+DMFT, which merges the local density approximation (LDA) with dynamical mean field theory (DMFT). With a fixed value of the Coulomb $U = 6.0$ eV, we show how the abrupt pressure driven MIT is understood in a new picture: pressure-induced decrease of the trigonal distortion within the strong correlation scenario (which is not obtained within LDA). We find good quantitative agreement with (i) switch of the orbital occupation of $(a_{1g}, e_{g1}^\pi, e_{g2}^\pi)$ and the spin state $S = 1$ across the MIT, (ii) thermodynamics and *dc* resistivity, and (iii) the one-electron spectral function, within this new scenario.

PACS numbers: 71.28+d, 71.30+h, 72.10-d

The spectacular metal-insulator transition (MIT) in the paramagnetic (P) state in V_2O_3 has long been considered as a classic, and by now almost a textbook version of correlation-driven MIT in a one-band correlated system described by the one-band Hubbard model [1]. This conventional wisdom has been recently challenged by new experiments, clearly showing the coupled spin-orbital character of the system, and necessitating a revision in terms of a multiband picture.

The conventionally accepted picture rested upon the following argument. In the high- T phase, V_2O_3 exists in the corundum structure, and with a $3d^2$ state (V^{3+}), the two e_g^σ orbitals are empty, while the triply degenerate t_{2g} orbitals are filled by two electrons. This triple degeneracy is lifted by a small trigonal distortion, leading to a singly occupied a_{1g} orbital oriented along the c -axis, and doubly degenerate planar e_g^π orbitals, occupied by the second electron. Castellani *et al.* [2] proposed that strong covalent effects lead to a bonding singlet a_{1g} state involving two V ions along the c -axis. The remaining electron in the two-fold degenerate e_g^π orbitals gives rise to a $S = 1/2$ model with orbital degeneracy. This inspired development of theoretical techniques, culminating in the dynamical mean field theory (DMFT) [3], leading to considerable improvement in our understanding of the MIT. Within the basic picture [2], Rozenberg *et al.* [4] used DMFT for one- and two-orbital Hubbard models with Bethe density-of-states to study the MIT in V_2O_3 .

Recent polarized X-ray scattering results of Park *et al.* [5] require, however, an interpretation in terms of a spin $S = 1$ at each V site, with a mixed orbital $e_g^\pi a_{1g} : e_g^\pi e_g^\pi = x : (1-x)$ configuration. An exciting conclusion from these results is that the above ratio changes its value *abruptly* at the MIT, forcing one to abandon the one-band Hubbard model to describe V_2O_3 . Notice that this implies an important role for the trigonal splitting, since the lower-lying orbital will be more “localized” when local Coulomb interactions are switched on. This raises questions concerning a possible link between the or-

bital “switching” and the drastic change in the electronic state, and to a possible common underlying origin.

The high-spin ground state results from strong Hund coupling, a fact borne out by LDA+U [6]. Furthermore, LDA+U results argue in favor of models without orbital degeneracy. This line of thought has been extended in detail by Tanaka [7], including spin-orbit coupling effects in a cluster-based approach. Mila *et al.* [8] have proposed a model with $S = 1$ and orbital degeneracy for the antiferromagnetic insulating phase.

Hallmarks of strong electronic correlations in V_2O_3 have been observed across the MIT in thermodynamic [9], *dc* transport [10], photoemission [11], and optical [12] responses. In particular, specific heat measurements give $\gamma_{el} \simeq 4.4$, $\rho_{dc}(T) = \rho_0 + AT^2$ with large A in the PM phase, while PES and optical measurements clearly reveal gap formation in the PI phase, and the development of low-energy quasicohherent weight in the PM, with a dynamical spectral weight transfer (SWT) from high- to low energy over a wide energy scale ($\simeq 4$ eV). This type of dynamical SWT-driven MIT is beyond the scope of LDA+U, which treats dynamical effects of local Coulomb interactions within static Hartree-Fock (HF) approximation. These are precisely the effects captured reliably by DMFT.

Thus, a consistent description of the MIT, along with an understanding of the strong correlation features requires a combination of structural aspects of V_2O_3 (encoded in LDA+U) with a reliable many-body theory like DMFT. In this letter, we study these questions within LDA+DMFT [13], which has been shown to provide a good quantitative *ab-initio* description of correlated electronic systems. Moreover the MIT in the P-phase has been studied [13] using LDA+DMFT(QMC). However, the link between the MIT and the abrupt switching of orbital occupation has, to our knowledge, not been explored in detail. We should mention that such a scenario may have broader application to other systems, notably in $Ca_{2-x}Sr_xRuO_4$ [14], and is a hallmark of the

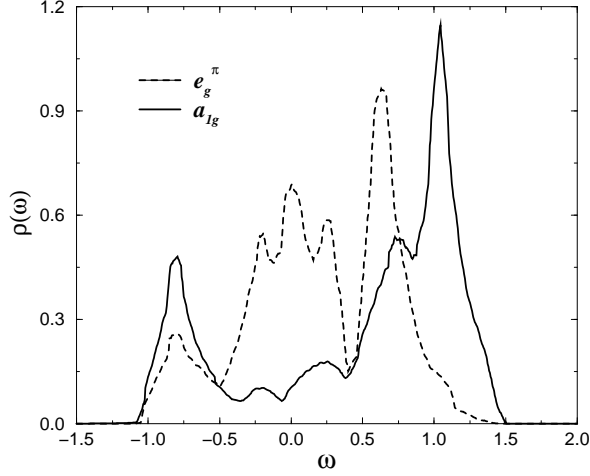


FIG. 1. LDA partial density of states for the e_g^π (dashed) and a_{1g} (solid) orbitals, obtained from Ref. [13].

importance of orbital correlations in a system.

We start with the actual LDA bandstructure of V_2O_3 in the corundum structure [13]. These results represent (Fig. 1) metallic behavior, with comparable width (2.5 eV) for both a_{1g} and e_g^π bands, and a strongly asymmetric structure. With an onsite $U \simeq 5 - 6$ eV, this would invalidate a MO-based approach [6]. Further from the $a_{1g} - e_g^\pi$ splitting, the trigonal field splitting is estimated to be $\simeq 0.4$ eV. The LDA densities of states with and without the trigonal distortion do not differ much, and in fact are both representative of good metallic behavior, showing that the MIT cannot be related purely to Δ_{trg} . Notice that at the local level, external pressure decreases Δ_{trg} , resulting in a sudden increase in $n_{a_{1g}}$ around $\Delta_{trg} = 0.28$ eV [7]. Turning on the local interactions, U, J_H and $U' = (U - 2J_H)$ will push up most of the spectral weight to the Hubbard sub-bands, and strong J_H will favor $S = 1$ at each V site. So, while these “ground state” features are reasonably well accounted for by LDA(+U), aspects like the mixed orbital configuration, the switch in orbital occupation at the MIT accompanied by dynamical SWT require a reliable treatment of dynamics of correlated electrons.

Thus, the one-particle part (LDA) of the Hamiltonian is

$$H_0 = \sum_{\mathbf{k}\alpha\beta\sigma} \epsilon_{\alpha\beta}(\mathbf{k}) c_{\mathbf{k}\alpha\sigma}^\dagger c_{\mathbf{k}\beta\sigma} \quad (1)$$

with the total DOS, $\rho_{total}^0(\epsilon) = \sum_{\mathbf{k}\alpha\beta\sigma} \delta(\epsilon - \epsilon_{\alpha\beta}(\mathbf{k}))$, and $\alpha, \beta = a_{1g}, e_{g1}^\pi, e_{g2}^\pi$. To avoid double counting of interactions which are already treated on the average by LDA, we follow [13] to write

$$H_{LDA}^0 = \sum_{\mathbf{k}\alpha\beta\sigma} \epsilon_{\alpha\beta}(\mathbf{k}) c_{\mathbf{k}\alpha\sigma}^\dagger c_{\mathbf{k}\beta\sigma} + \sum_{i\alpha\sigma} \epsilon_{i\alpha\sigma}^0 n_{i\alpha\sigma}, \quad (2)$$

where $\epsilon_{i\alpha\sigma}^0 = \epsilon_{i\alpha\sigma} - U(n_{\alpha\sigma} - \frac{1}{2}) + \frac{1}{2}J_H(n_{\alpha\bar{\sigma}} - 1)$, with U, J_H as defined below.

With the interactions in the t_{2g} sector, the full Hamiltonian reads,

$$H = H_0 + U \sum_{i\alpha} n_{i\alpha\uparrow} n_{i\alpha\downarrow} + \sum_{i\alpha\beta\sigma\sigma'} U_{\alpha\beta}^{\sigma\sigma'} n_{i\alpha\sigma} n_{i\beta\sigma'}. \quad (3)$$

Constrained LDA calculations yield $U = 5 - 6$ eV (without inclusion of screening of t_{2g} interactions by e_g electrons), $J_H \simeq 1$ eV, and $U_{\alpha\beta}^{\sigma\sigma'} \equiv U' = (U - 2J_H) = 3 - 4$ eV. Following [13], we use the fact that the e_g^π bands are well separated from the t_{2g} bands to consider only the t_{2g} manifold. Furthermore, in the PM and para-orbital phase, we have $G_{\alpha\beta\sigma\sigma'}(\omega) = \delta_{\alpha\beta}\delta_{\sigma\sigma'}G_{\alpha\sigma}(\omega)$ and $\Sigma_{\alpha\beta\sigma\sigma'}(\omega) = \delta_{\alpha\beta}\delta_{\sigma\sigma'}\Sigma_{\alpha\sigma}(\omega)$.

In the t_{2g} sub-basis, a DMFT solution involves (i) replacing the lattice model by a self-consistently embedded multi-orbital, asymmetric Anderson impurity model, and (ii) a selfconsistency condition which requires the impurity propagator to be equal to the local (k -averaged) Green function of the lattice, given by

$$G_\alpha(\omega) = \frac{1}{V_B} \int d^3k \left[\frac{1}{(\omega + \mu)1 - H_{LSDA}^0(\mathbf{k}) - \Sigma(\omega)} \right]_\alpha. \quad (4)$$

Using the locality of $\Sigma_{\alpha\beta}$ in $d = \infty$, we have $G_\alpha(\omega) = G_\alpha^0(\omega - \Sigma_\alpha(\omega))$ from the Hilbert transform of the LDA DOS. Also, importantly, the inter-orbital couplings scatter electrons between the a_{1g}, e_g^π bands, so that only the total number, $n_{t_{2g}} = \sum_\alpha n_{t_{2g},\alpha}$ is conserved in a way consistent with Luttinger’s theorem.

To solve the multi-orbital, asymmetric Anderson impurity problem, we use the iterated perturbation theory (IPT), suitably generalized to the case of t_{2g} orbitals for arbitrary filling [15]. The local propagators are given by

$$G_\alpha(\omega) = \frac{1}{N} \sum_{\mathbf{k}} \frac{1}{\omega - \Sigma_\alpha(\omega) - \epsilon_{\mathbf{k}\alpha}}. \quad (5)$$

Local self-energies $\Sigma_\alpha(\omega)$ are computed within an extended IPT scheme that explicitly satisfies the generalized Friedel sum rule (Luttinger’s theorem) to a very good accuracy. Mathematically,

$$\Sigma_\alpha(\omega) = \frac{\sum_\gamma A_{\alpha\gamma} \Sigma_{\alpha\gamma}^{(2)}(\omega)}{1 - \sum_\gamma B_{\alpha\gamma} \Sigma_{\alpha\gamma}^{(2)}(\omega)} \quad (6)$$

where, for example,

$$\Sigma_{\alpha\gamma}^{(2)}(i\omega) = N_{\alpha\gamma} \frac{U_{\alpha\gamma}^2}{\beta^2} \sum_{nm} G_\alpha^0(i\omega_n) G_\gamma^0(i\omega_m) G_\gamma^0(i\omega_n + i\omega_m - i\omega) \quad (7)$$

with $N_{\alpha\gamma} = 2$ for $\alpha, \gamma = e_{g1}^\pi, e_{g2}^\pi$ and 4 for $\alpha, \gamma = a_{1g}, e_{g1,2}^\pi$. The bath propagator is $G_\alpha^0(\omega) = [\omega + \mu_\alpha -$

$\Delta_\alpha(\omega)]^{-1}$. In the above, $A_{\alpha\gamma} = \frac{n_\alpha(1-2n_\alpha)+D_{\alpha\gamma}[n]}{n_\alpha^0(1-n_\alpha^0)}$ and $B_{\alpha\gamma} = \frac{(1-2n_\alpha)U_{\alpha\gamma}+\epsilon_\alpha-\mu_\alpha}{2U_{\alpha\gamma}^2 n_\alpha^0(1-n_\alpha^0)}$. Also, n_α and n_α^0 are particle numbers defined from G_α and G_α^0 , and the inter-orbital correlation function is $D_{\alpha\gamma}[n] = \langle n_\alpha n_\gamma \rangle = \langle n_\alpha \rangle \langle n_\gamma \rangle - \frac{1}{U_{\alpha\gamma}\pi} \int_{-\infty}^{+\infty} f(\omega) \text{Im}[\Sigma_\alpha(\omega)G_\alpha(\omega)]d\omega$. This last identity follows directly from the equation of motion for $G_\alpha(\omega)$.

These coupled equations are solved selfconsistently to obtain the spectral function. We choose $\Delta_{trg} \simeq 0.32$ eV, completely consistent with the LDA. To study the MIT, we notice that external pressure decreases the quantity $\Delta_{trg} = E_{a_{1g}} - E_{e_g^\pi}$ and leads to an increase in $n_{a_{1g}}$; in particular, it leads to a reduction in Δ_{trg} across 0.28, at which point, a sudden increase in $n_{a_{1g}}$ has been reported from cluster calculations [7]. To study this effect, we monitor the spectral function for different values of $n_{a_{1g}}$, with fixed total number of electrons.

In Fig. 2, we show the partial DOS for the e_g^π, a_{1g} orbitals, for the metallic (dashed) and “Mott” insulating (solid) phases, corresponding to total a_{1g} occupation $n_{a_{1g}} = 0.41, 0.36$, respectively. As expected from the trigonal splitting assignment, the lower-lying e_g^π orbitals are more localized in the solid, with a gap, $\Delta_{e_g^\pi} = 0.45$ eV. Correspondingly, the a_{1g} band is more itinerant, completely consistent with the fact that $t_{a_{1g}, a_{1g}}$ is by far the largest hopping integral in the real system. From Fig. 2, we estimate $\Delta_{Ins} = 0.35$ eV. With $n_{a_{1g}} = 0.41$, the e_g^π spectral function still exhibits insulator-like features, while the a_{1g} spectrum develops a very narrow, quasicohherent peak with a $FWHM = 0.07$ eV at E_F . We interpret these results as a microscopic derivation of the phenomenological “two-fluid” models proposed earlier to understand metal-insulator transitions [3]. In our new picture, increasing pressure decreases Δ_{trg} , resulting in increased population of the a_{1g} orbital, and leading (via $t_{a_{1g}, a_{1g}}$) to an abrupt MIT accompanied by large dynamical SWT.

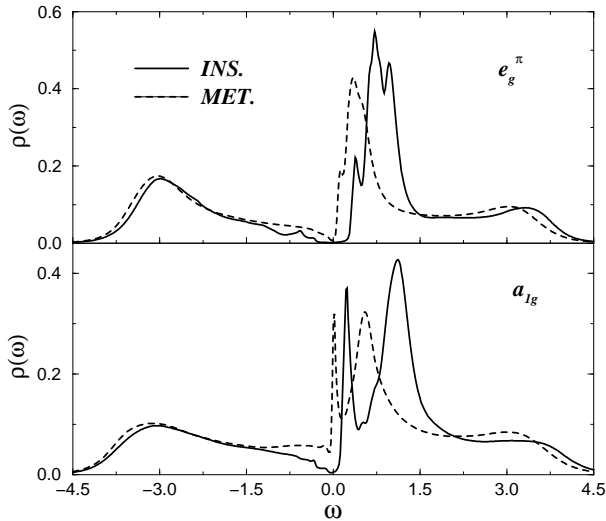


FIG. 2. t_{2g} partial density of states using LDA+DMFT for $U = 6.0$ eV in the PI (solid) and PM (dashed) phases of V_2O_3 .

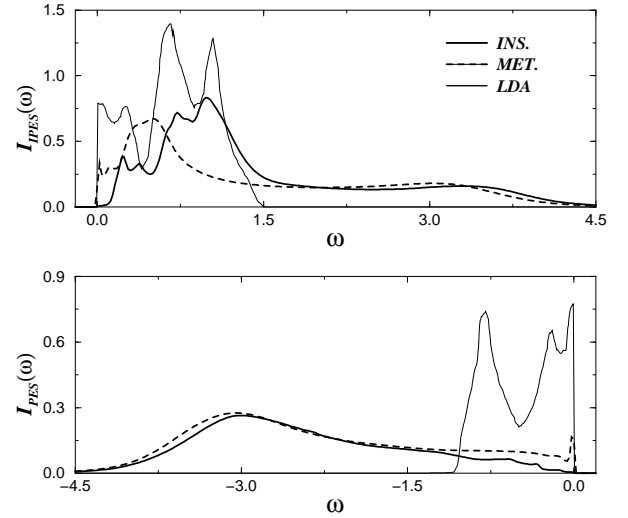


FIG. 3. The integrated inverse- and direct photoemission lineshapes for the PI (solid) and PM (dashed) phases within LDA+DMFT for $U = 6.0$ eV. The LDA result is the thin solid line.

mical SWT.

Using the corresponding self-energy, we carry out a quantitative estimate for the effective mass enhancement and the A -coefficient of the low- T quadratic term in the dc resistivity. Indeed, from $\text{Re}[\Sigma_{a_{1g}}(\omega)]$, we estimate

$m^*/m = [1 - \frac{\partial \Sigma'_{a_{1g}}(\omega)}{\partial \omega}]^{-1} = 4.16$, close to the value of 4.4 extracted from low- T specific heat measurements. Also, $A = \rho_{dc}(T)/T^2 = (m^*/ne^2)|\partial^2 \Sigma'_{a_{1g}}(\omega)/\partial \omega^2|$ is large, because $|\partial^2 \Sigma'_{a_{1g}}(\omega)/\partial \omega^2| = 38 \gg 1$. This will result in a large quadratic term in the low- T dc resistivity, as observed.

In Fig. 3, we show the integrated PES and IPES spectra in the metallic and insulating phases, along with the corresponding LDA spectra. As one would expect, and consistent with observations, the PES spectrum shows a very narrow quasicohherent peak, with most of the spectral weight in the incoherent “lower Hubbard band”, centered at $\omega = -3.0$ eV. The PES intensity at E_F is strongly reduced from the LDA prediction. Quantitative comparison with the PES spectra measured at higher T needs an extension of our approach to finite T ; however, we expect that the strong T -dependence of the quasicohherent feature within DMFT will smear out the low-energy peak for $T > T_{coh} \simeq 300K$, bringing the spectra in closer agreement with published PES results. Signatures of strong correlations are also visible in the IPES spectra as “upper Hubbard band” features, and the difference between the LDA and LDA+DMFT spectra is striking.

Especially interesting is the change in the spectral function at E_F as a function of $n_{a_{1g}}$. In Fig. 4, we show this variation for our chosen parameter set. Astonishingly, $\rho(E_F)$ exhibits a sharp jump from 0 to 0.261

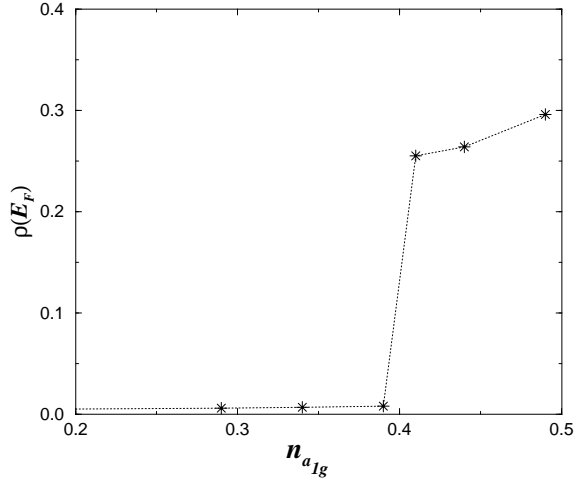


FIG. 4. The total DOS at E_F as a function of the a_{1g} orbital occupation.

around $n_{a_{1g}} = 0.39$, clearly showing that the MIT is indeed first order, in agreement with observations. Our results imply that the MIT is accompanied by an abrupt jump in the itinerant carrier density, rather than increase in carrier mobility, and is consistent with the conductivity jump at the PI-PM transition. From the computed spectral functions, $(n_{a_{1g}}, n_{e_{g1}^\pi}, n_{e_{g2}^\pi}) = (0.36, 0.82, 0.82)$ in the PI, and $(0.41, 0.79, 0.79)$ in the PM. Our calculated orbital occupations are slightly different from those estimated by polarized XAS measurements [5], but show the correct trend across the MIT. Further, we find $\langle S_{iz}^2 \rangle = \frac{1}{4} \sum_{\alpha} \langle [n_{i\alpha\uparrow} - n_{i\alpha\downarrow}]^2 \rangle = 0.92$ for the chosen parameter set, consistent with the observation of $S = 1$ at each V site. Finally, we monitor D_{a_{1g}, e_{g1}^π} and $D_{e_{g1}^\pi, e_{g2}^\pi}$ and find that both *decrease* across the MIT: in fact, $D_{a_{1g}, e_{g1}^\pi} = -0.043$ for $n_{a_{1g}} = 0.36$ (PI), and equals -0.007 for $n_{a_{1g}} = 0.41$ (PM), while $D_{e_{g1}^\pi, e_{g2}^\pi} = -0.065$ (PI) and -0.036 (PM) showing clearly that the MIT is accompanied by a strong *reduction* of local (anti-ferro) orbital correlations.

As mentioned earlier, the MIT in V_2O_3 has recently been studied [13] by LDA+DMFT(QMC), so it is instructive to compare our approach with theirs. Though QMC is numerically exact, it cannot access the low- T regime ($T < 400K$). Further, analytic continuation of Matsubara (imaginary) frequencies onto the real frequencies is a highly ill-posed numerical problem. While the IPT is not exact, it is free from these drawbacks, and is known to yield reliable results for the problem at hand [15], enabling one to study thermodynamic and transport properties at relatively modest computational cost. In contrast to the earlier pioneering study, we have explicitly shown the existence of the first-order PI-PM transition and its intimate link to the accompanying orbital switching in V_2O_3 . We have not attempted

to make a detailed comparison with finite- $T > 170K$ spectral functions in the PI and PM regions, a program which has been carried out in Ref. [13] (but only for $T > 400 K$, where the first-order MIT is replaced by a smooth crossover), and we plan to report these aspects, along with finite- T transport properties and lattice effects, in a future work.

In conclusion, we have presented a different scenario, based on combination of LDA bandstructure with dynamical, local spin and orbital correlations, to understand salient features of the first-order MIT in the P-phase of V_2O_3 . The first-order MIT is shown to be accompanied by changes in orbital occupation in a way qualitatively consistent with observations. Further, very good agreement with low- T thermodynamic and *dc* resistivity is obtained within the same approach. This represents a new picture for the correlation-driven MIT in V_2O_3 ; one which has applications to other systems where coupled spin-orbital correlations result in changes in orbital occupations across the MIT. Such an approach should be applicable, with extensions to include broken symmetries in the spin/orbital sectors, to systems like $Ca_{2-x}Sr_xRuO_4$ as well.

We are indebted to L. H. Tjeng for many enlightening discussions. Work carried out with the support of the Sonderforschungsbereich 608 of the Deutsche Forschungsgemeinschaft.

-
- [1] M. Imada, A. Fujimori and Y. Tokura, Rev. Mod. Phys. **70**, 1039 (1998).
 - [2] C. Castellani, A. Natoli and J. Ranninger, Phys. Rev. B **18**, 4945 (1978); **18**, 4967 (1978); **18**, 5001 (1978).
 - [3] A. Georges, G. Kotliar, W. Krauth and M. Rozenberg, Rev. Mod. Phys. **68**, 13 (1996), and references therein.
 - [4] M. Rozenberg *et al.*, Phys. Rev. Lett. **69**, 1236 (1992); **75**, 105 (1995).
 - [5] J. Park *et al.*, Phys. Rev. B **61**, 11506 (2000).
 - [6] S. Yu Ezhov *et al.*, Phys. Rev. Lett. **83**, 4136 (1999).
 - [7] A. Tanaka, J. Phys. Soc. Jpn. **71**, 1091 (2002).
 - [8] F. Mila *et al.*, Phys. Rev. Lett. **85**, 1714 (2000).
 - [9] L. F. Mattheiss, J. Phys. Condens. Matter, **6**, 6477 (1994).
 - [10] S. A. Shivashankar and J. M. Honig, Phys. Rev. B **28**, 5695 (1983), and references therein.
 - [11] J. Park, Ph.D thesis, University of Michigan (1994).
 - [12] G. A. Thomas *et al.*, Phys. Rev. Lett. **73**, 1529 (1994).
 - [13] K. Held *et al.*, Phys. Rev. Lett. **86**, 5345 (2001).
 - [14] S. Nakatsuji *et al.*, J. Phys. Soc. Jpn. **66**, 1868 (1997).
 - [15] S. V. Savrasov, G. Kotliar and E. Abrahams, Nature **410**, 793 (2001).